PROCEEDINGS OF SPIE

SPIEDigitalLibrary.org/conference-proceedings-of-spie

Dispersion behavior of a hybrid phononic resonator

D. DePauw, H. Al Ba'ba'a, M. Nouh

D. DePauw, H. Al Ba'ba'a, M. Nouh, "Dispersion behavior of a hybrid phononic resonator," Proc. SPIE 10600, Health Monitoring of Structural and Biological Systems XII, 1060014 (27 March 2018); doi: 10.1117/12.2296656

Event: SPIE Smart Structures and Materials + Nondestructive Evaluation and Health Monitoring, 2018, Denver, Colorado, United States

Dispersion behavior of a hybrid phononic resonator

D. DePauw[a], H. Al Ba'ba'a[a], and M. Nouh[a]

[a]Mechanical and Aerospace Engineering Dept., SUNY at Buffalo, Buffalo, USA

ABSTRACT

Considerable research attention has been recently devoted to the study of periodic structures given their unique wave dispersion. Phononic crystals and acoustic metamaterials have emerged as two main categories of such periodic structures that can exhibit radically different band gap characteristics. Here, we present a novel configuration that combines hybrid wave attenuation attributes culminating in enhanced metadamping and energy dissipation properties. The results are compared with a benchmark example from literature to show the potential of the new design.

Keywords: Metamaterial, metadamping, phononic, band gap

1. INTRODUCTION

The development of periodic structures was intended for solid state and optical applications[1–5] and has been expanded to include hierarchical mechanical systems including discrete spring-mass lattices, composite beams, and flexural plates.[6–15] Such periodic structures can be categorized into two main categories: Phononic Crystals (PCs) (Figure 1a) and Acoustic Metamaterials (AMs) (Figure 1b). In the simpler discrete cell mode, the unit cell of a PC exhibits a periodic change in material or geometrical properties, or a combination thereof. Owing to their periodic nature, waves propagating within certain frequency ranges fail to propagate in the periodic medium due to impedance mismatches caused by Bragg scattering effects. Such frequency ranges are referred to as band gaps.[16,17] On the other hand, AMs are another class of periodic structures that comprise locally resonant components which are supported by by the outer (host) structure. Such a configuration creates band gaps at a subwavelength scale which, as a result, can be tuned to considerably lower frequencies.[18–25] Band gaps in AMs occur near the natural frequencies of the resonators due to the emergence of a negative effective mass.[26] As such, these band gaps are solely dependent on the mechanical properties of the local resonance source, which provides more design flexibility.

In this paper, a new model is proposed which exhibits qualitative properties of both PCs and AMs. The new system, referred to herein as a Phononic Resonator (PR) (Figure 1c), comprises a unit cell which contains a non-local resonating component. The cell contains two discrete masses, m_a and m_b. The neighboring m_a masses are connected via a spring k_a, while a resonator mass m_b is sandwiched between each two m_a masses and is connected to them via two springs of stiffness k_b each. A PR structure, given the appropriate choice of parameters, can exhibit both Bragg scattering and local resonance band gaps. Further, the PR is shown to generate higher metadamping (i.e. larger damping ratios with the same amount of damping) which can outperform both AMs and PCs.[27]

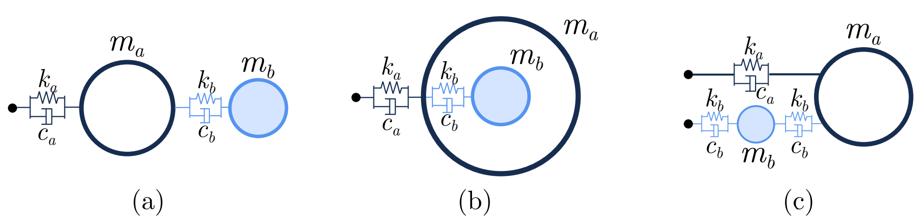

Figure 1. Unit cell of (a) Phononic Crystal (PC), (b) Acoustic Metamaterial (AM), and (c) Phononic Resonator (PR)

Further author information: (Send correspondence to M. Nouh)
E-mail: mnouh@buffalo.edu

Health Monitoring of Structural and Biological Systems XII, edited by Tribikram Kundu, Proc. of SPIE Vol. 10600, 1060014 · © 2018 SPIE · CCC code: 0277-786X/18/$18 · doi: 10.1117/12.2296656

2. UNDAMPED DISPERSION RELATION

A dispersion curve is the relationship between the wave number β of a propagating wave and the excitation frequency ω. This relationship can be used to identify band gaps as regions where a frequency solution that corresponds to a real wave number does not exist. Here, we show the development of the dispersion relation for the PR, since the AM and PC counterparts are well established.[27,28] To derive the dispersion relation, we obtain equations of motion of a PR unit cell as follows:

$$m_a\ddot{u}_i + c_a(2\dot{u}_i - \dot{u}_{i+1} - \dot{u}_{i-1}) + k_a(2u_i - u_{i+1} - u_{i-1}) - c_b(\dot{v}_{i+1} + \dot{v}_i - 2\dot{u}_i) - k_b(v_{i+1} + v_i - 2u_i) = 0 \tag{1a}$$

$$m_b\ddot{v}_i + 2c_b\dot{v}_i + 2k_bv_i - c_b(\dot{u}_{i-1} + \dot{u}_i) - k_b(u_{i-1} + u_i) = 0 \tag{1b}$$

We first consider the undamped case where $c_a = c_b = 0$. Upon substituting the Bloch theorem[29] into the undamped PR equations of motion, the dispersion relation is found by solving the eigenvalue problem to get:

$$m_am_b\omega^4 - 2(k_b(m_b + m_a) + k_am_b(1 - \cos\bar{\beta}))\omega^2 + (4k_ak_b + 2k_b^2)(1 - \cos\bar{\beta}) = 0 \tag{2}$$

The dispersion relation can then be normalized using $\Omega = \frac{\omega}{\omega_0}$ where $\omega_0 = \sqrt{\frac{k_b}{m_b}}$ and cast in a non-dimensional form:

$$\Omega^4 - (2(1+\mu) + \frac{2\mu}{\kappa}(1 - \cos\bar{\beta}))\Omega^2 + (\frac{4\mu}{\kappa} + 2\mu)(1 - \cos\bar{\beta}) = 0 \tag{3}$$

where $\mu = \frac{m_b}{m_a}$, $\kappa = \frac{k_b}{k_a}$, and $\bar{\beta}$ is the dimensionless wavenumber. Eq. (3) represents the free-wave formulation of the dispersion relation, where the wave number is swept over the irreducible Brillouin zone ($\bar{\beta} \in [0, \pi]$). The driven-wave formulation, on the other hand, produces the wave number as a function of the frequency, i.e. $\bar{\beta}(\omega)$, which can be found by reformulating Eq. (3) as $\bar{\beta} = \cos^{-1}\Phi(\Omega)$ such that:

$$\Phi(\Omega) = 1 - \frac{\kappa}{2\mu}\frac{\Omega^4 - 2(1+\mu)\Omega^2}{\Omega^2 - (2+\kappa)} \tag{4}$$

Upon inspection of the dispersion relation in Eq. (3), it is noticed that the optic band can be manipulated to resemble either the optic band structure of a PC or AM with a variation of the system parameters. The optic branch of an AM has a positive group velocity and that of the PC has a negative one. Given that a PR can mimic both the AM and the PC, a turning point for the optic branch has to exist where the non-zero solution of the dispersion relation at $\bar{\beta} = 0$ is equal to the a solution at $\bar{\beta} = \pi$ as an indication of a flat optic branch. Substituting back into Eq. (3), it can be shown that the turning condition is satisfied if $2\mu = \kappa$ where the optic dispersion branch is flat and the group velocity will be equal to zero. For $2\mu > \kappa$, the optic band behaves in a manner consistent with AM and posses a positive group velocity, while for $2\mu < \kappa$ the optic band resembles the optic band of a PC with a negative group velocity. As a special case, the PR system can also resemble a homogeneous lattice with no band gap if $\mu = \frac{\kappa}{2+\kappa}$. These cases are graphically summarized in Figure 2.

The PR is also capable of creating attenuation that resembles both PC and AM designs (as seen from the imaginary component of $\bar{\beta}$ in Figure 2). An anti-resonance frequency, $\hat{\Omega}_R = \sqrt{2+\kappa}$, can occur within the band gap when the PR behaves similar to an AM. This anti-resonance can be found by setting the denominator of $\Phi(\omega)$ in Eq. (4) to zero; yielding unbounded attenuation $\Im[\bar{\beta}]$ as expected from an AM-like behavior.[30] The PR can also have band gaps caused purely by Bragg scattering if the anti-resonance $\bar{\beta}$ frequency occurs outside the range of the band gap (Figure 2).

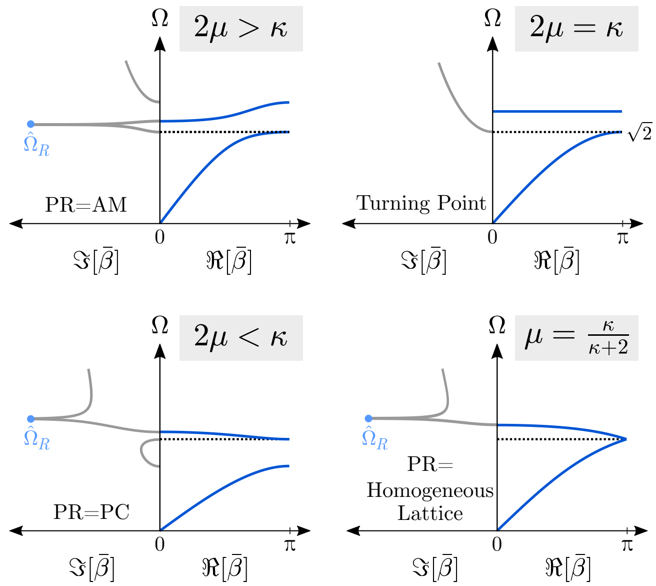

Figure 2. Dispersion diagram of the Phononic Resonator (PR) at different combinations of the mass and stiffness ratios

3. DAMPING PROPERTIES OF PR

To analyze the damping properties of a phononic resonator, dampers are inserted into the model parallel to each spring, and labeled c_a and c_b. A new dispersion relation for PR that includes these dampers can be derived using a similar methodology as presented earlier, which can be shown to be:

$$\lambda^4 + a\lambda^3 + b\lambda^2 + c\lambda + d = 0 \tag{5}$$

where:

$$a = \frac{2c_b(m_a + m_b) + 2c_a m_b(1 - \cos\bar{\beta})}{m_a m_b} \tag{6a}$$

$$b = \frac{2k_b(m_a + m_b) + 2(k_a m_b + 2c_a c_b + c_b^2)(1 - \cos\bar{\beta})}{m_a m_b} \tag{6b}$$

$$c = \frac{4(c_a k_b + k_a c_b + c_b k_b)(1 - \cos\bar{\beta})}{m_a m_b} \tag{6c}$$

$$d = \frac{2k_b(2k_a + k_b)(1 - \cos\bar{\beta})}{m_a m_b} \tag{6d}$$

The equivalent dispersion relations for damped AM and PC can be found in literature.[27,28] A solution of the dispersion relations takes the following form:

$$\lambda_s(\beta) = -\xi_s(\beta)\omega_s(\beta) \pm \omega_{d_s}(\beta), \quad s = 1, 2 \tag{7}$$

where ω_{d_s} is the damped resonant frequency of the system, and $s = 1, 2$ refers to the acoustic and optic dispersion branches, respectively. ξ_s is the damping ratio for a given wave number and can be calculated using $\xi_s(\beta) = -\Re[\xi_s(\beta)]/\mathrm{Abs}[\xi_s(\beta)]$, while ω_s is the undamped resonant frequency. The differences in ξ_s across the wave number spectrum when comparing different designs with like-valued dampers is an effect of the metadamping phenomenon. Designs with higher damping ratios across the wave number spectrum can attenuate incident waves more efficiently with the same amount of material damping compared to those with lower damping ratios.

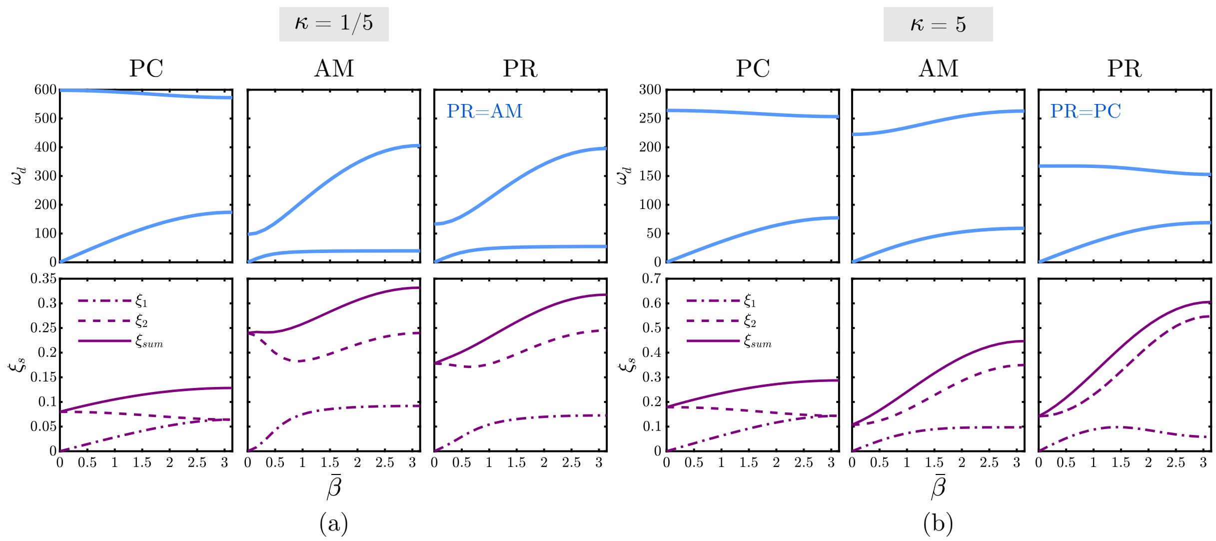

Figure 3. Dispersion diagram of a damped PR, AM, and PC with a mass ratio of $\mu = 5$ and stiffness ratios of (a) $\kappa = 1/5$ and (b) $\kappa = 5$

In order to accurately compare different models, it must first be ensured that the systems are statically equivalent, meaning that they all must have the same long wave speed, or that their acoustic dispersion branches have the same initial slope (c_{stat}). To ensure a fair comparison, we use a benchmark example from literature with the following set of parameters: $m_a = 1$ and $k_a = 1$, $m_b = 5$ (i.e. $\mu = 5$), $\kappa = 1/5$, $\omega_0^{\mathrm{PC}} = 100$, and $\omega_0^{\mathrm{AM}} = 40.9$. For an equivalent c_{stat} of PR, the adjusted ω_0^{PR} is equal to 38.9 resulting in a long wave speed of $c_{stat} = 83.3$ for all three models. The damping coefficients $c_a = c_b = 40$ are used for all three systems. However, since the PR has three dampers in each unit cell as compared to an AM and a PC, the value of c_b is halved. Figure 3 shows the damping ratios across the optic and acoustic bands for the benchmark examples (Figure 3a) as well as for the same parameters but with $\kappa = 5$ (Figure 3b). As can be seen from Figure 3, increasing the stiffness ratio gives the PR a higher damping ratio when compared to the AM and the PC. Although the PR behaves as a PC at $\kappa = 5$, the damping ratios are higher than those of the AM (which have typically demonstrated larger metadamping effects[27]).

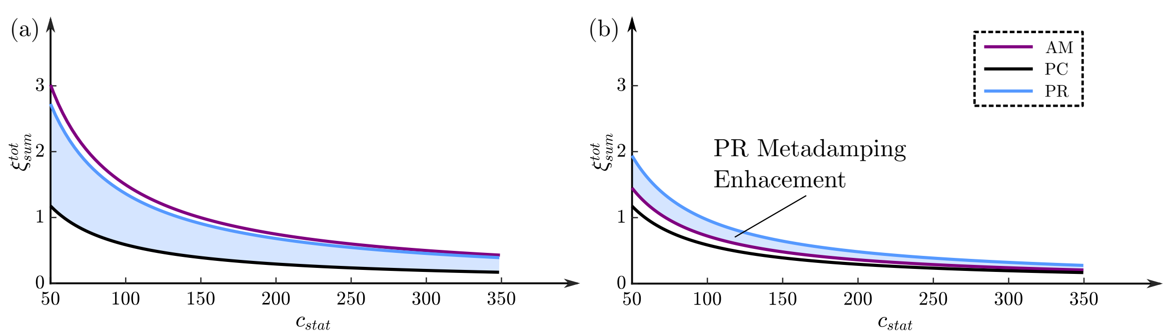

Figure 4. Metadamping comparison as a function of c_{stat} for $\mu = 5$ and (a)$\kappa = 1/5$ and (b) $\kappa = 5$

ξ_{sum} in Figure 3 is a metric of the total damping ratio across both the optic and acoustic branch for each model, and can be found using $\xi_{sum}(\beta) = \xi_1(\beta) + \xi_2(\beta)$. The summed damping ratio ξ_{sum} for each model can be integrated over wave numbers ranging from 0 to π to give a metadamping metric ξ_{sum}^{tot}. If c_{stat} is swept over a range of values while keeping the same mass and stiffness ratios (by changing the value of ω_0), a graph can be constructed to view the differences in effective metadamping across all the c_{stat} values. Figure 4 shows ξ_{sum}^{tot} as a function of c_{stat} for all three models where higher values of ξ_{sum}^{tot} imply enhanced metadamping effects. In both Figures 4a and 4b, the PR clearly outperforms the PC in terms of total metadamping. For Figure 4a, the

AM has slightly higher total metadamping than PR. However, as in the case of Figure 4b, the PR has higher total metadamping than both AM and PC. This confirms the trend observed in Figure 3 where a PR is capable of exhibiting a larger metadamping effect than that of the AM given the right choice of parameters.

4. CONCLUSION

The phononic resonator (PR) is a hybrid design that exhibit characteristics of both phononic crystals (PCs) and acoustic metamaterials (AMs). The unique ability of the PR dispersion curve to behave similar to either AM or PC allows for greater flexibility in the design of metamaterials as well as their tunability. The PR design has also been shown to exhibit larger metadamping effects for the same damping values when compared to equivalent AM and PC designs and given the suitable choice of parameters.

REFERENCES

[1] Veselago, V. G., "the Electrodynamics of Substances With Simultaneously Negative Values of ϵ and μ," *Soviet Physics Uspekhi* **10**(4), 509–514 (1968).

[2] Smith, D. R., Pendry, J. B., and Wiltshire, M. C. K., "Metamaterials and Negative Refractive Index," *Science* **305**(August), 788–792 (2004).

[3] Jaggard, D. L., Mickelson, A. R., and Papas, C. H., "On electromagnetic waves in chiral media," *Applied Physics* **18**, 211–216 (2 1979).

[4] Lindell, I., Sihvola, A., and Kurkijarvi, J., "Karl F. Lindman: the last Hertzian, and a harbinger of electromagnetic chirality," *IEEE Antennas and Propagation Magazine* **34**, 24–30 (6 1992).

[5] Ward, D. W., Nelson, K. A., and Webb, K. J., "On the physical origins of the negative index of refraction," *New Journal of Physics* **7**, 213–213 (10 2005).

[6] Mead, D., "Free wave propagation in periodically supported, infinite beams," *Journal of Sound and Vibration* **11**, 181–197 (2 1970).

[7] Cremer, L., Heckl, M., and Petersson, B., [*Structure-Borne Sound*], Springer Berlin Heidelberg, Berlin, Heidelberg (2005).

[8] Faulkner, M. G. and Hong, D. P., "Free vibrations of a mono-coupled periodic system," *Journal of Sound and Vibration* **99**(1), 29–42 (1985).

[9] Ruzzene, M., Scarpa, F., and Soranna, F., "Wave beaming effects in two-dimensional cellular structures," *Smart Materials and Structures* **12**, 363–372 (2003).

[10] Ruzzene, M. and Baz, A., "Control of Wave Propagation in Periodic Composite Rods Using Shape Memory Inserts," *Journal of Vibration and Acoustics* **122**(2), 151 (2000).

[11] Mead, D., "Wave propagation and natural modes in periodic systems: I. Mono-coupled systems," *Journal of Sound and Vibration* **40**, 1–18 (5 1975).

[12] Mead, D. and Markuš, ., "Coupled flexural-longitudinal wave motion in a periodic beam," *Journal of Sound and Vibration* **90**, 1–24 (9 1983).

[13] Mead, D. J., "Vibration Response and Wave Propagation in Periodic Structures," *Journal of Engineering for Industry* **93**(3), 783 (1971).

[14] Mead, D. J. and Yaman, Y., "The harmonic response of rectangular sandwich plates with multiple stiffening: A flexural wave analysis," *Journal of Sound and Vibration* **145**(3), 409–428 (1991).

[15] Sen Gupta, G., "Natural flexural waves and the normal modes of periodically-supported beams and plates," *Journal of Sound and Vibration* **13**, 89–101 (9 1970).

[16] Al Ba'ba'a, H., Nouh, M., and Singh, T., "Pole distribution in finite phononic crystals: Understanding bragg-effects through closed-form system dynamics," *The Journal of the Acoustical Society of America* **142**(3), 1399–1412 (2017).

[17] Al Ba'ba'a, H. B. and Nouh, M., "Mechanics of longitudinal and flexural locally resonant elastic metamaterials using a structural power flow approach," *International Journal of Mechanical Sciences* **122**, 341–354 (2017).

[18] Huang, H. H. and Sun, C. T., "A study of band-gap phenomena of two locally resonant acoustic metamaterials," *Proceedings of the Institution of Mechanical Engineers, Part N: Journal of Nanoengineering and Nanosystems* , 1740349911409981 (2011).

[19] Zhu, R., Liu, X., Hu, G., Sun, C., and Huang, G., "A chiral elastic metamaterial beam for broadband vibration suppression," *Journal of Sound and Vibration* **333**, 2759–2773 (5 2014).

[20] Baravelli, E. and Ruzzene, M., "Internally resonating lattices for bandgap generation and low-frequency vibration control," *Journal of Sound and Vibration* **332**(25), 6562–6579 (2013).

[21] Nouh, M., Aldraihem, O., and Baz, A., "Metamaterial structures with periodic local resonances," in [*Proc. SPIE*], Kundu, T., ed., **9064**, 90641Y (3 2014).

[22] Nouh, M., Aldraihem, O., and Baz, A., "Vibration Characteristics of Metamaterial Beams With Periodic Local Resonances," *Journal of Vibration and Acoustics* **136**(6), 61012 (2014).

[23] Nouh, M., Aldraihem, O., and Baz, A., "Wave propagation in metamaterial plates with periodic local resonances," *Journal of Sound and Vibration* **341**, 53–73 (2015).

[24] Al Ba'ba'a, H., Nouh, M., and Singh, T., "Formation of local resonance band gaps in finite acoustic metamaterials: A closed-form transfer function model," *Journal of Sound and Vibration* **410**, 429–446 (2017).

[25] Nouh, M., Aldraihem, O., and Baz, A., "Periodic metamaterial plates with smart tunable local resonators," *Journal of Intelligent Material Systems and Structures* **27**(13), 1829–1845 (2016).

[26] Huang, H. H., Sun, C. T., and Huang, G. L., "On the negative effective mass density in acoustic metamaterials," *International Journal of Engineering Science* **47**(4), 610–617 (2009).

[27] Hussein, M. I. and Frazier, M. J., "Metadamping: An emergent phenomenon in dissipative metamaterials," *Journal of Sound and Vibration* **332**(20), 4767–4774 (2013).

[28] Frazier, M. J., *Dissipative Wave Propagation in Phononic Crystals and Metamaterials: Models and Analysis*, PhD thesis, University of Colorado at Boulder (2015).

[29] Brillouin, L., [*Wave propagation in periodic structures; electric filters and crystal lattices*] (1946).

[30] Kulkarni, P. P. and Manimala, J. M., "Longitudinal elastic wave propagation characteristics of inertant acoustic metamaterials," *Journal of Applied Physics* **119**(24), 245101 (2016).